Title	Effect of acetyl substitution on the optical anisotropy of cellulose acetate films
Author(s)	Hatamoto, Kazuya; Shimada, Hikaru; Kondo, Misaki; Nobukawa, Shogo; Yamaguchi, Masayuki
Citation	Cellulose, 25(8): 4453-4462
Issue Date	2018-06-09
Type	Journal Article
Text version	author
URL	http://hdl.handle.net/10119/16121
Rights	This is the author-created version of Springer Nature, Kazuya Hatamoto, Hikaru Shimada, Misaki Kondo, Shogo Nobukawa, Masayuki Yamaguchi, Cellulose, 25(8), 2018, 4453-4462. The original publication is available at www.springerlink.com, http://dx.doi.org/10.1007/s10570-018-1890-4
Description	

Effect of acetyl substitution on the optical anisotropy of cellulose acetate films

Kazuya Hatamoto[1], Hikaru Shimada[1], Misaki Kondo[1],
Shogo Nobukawa[1,2], and Masayuki Yamaguchi[1*]

[1] School of Materials Science, Japan Advanced Institute of Science and Technology,
1-1 Asahidai, Nomi, Ishikawa 923-1292, JAPAN

[2] Department of Life Science and Applied Chemistry, Nagoya Institute of Technology,
Gokiso-cho, Showa-ku, Nagoya, Aichi 466-8555, JAPAN

***Corresponding Author**
M. Yamaguchi
Phone +81-761-51-1621
Fax +81-761-51-1149
e-mail m_yama@jaist.ac.jp

Abstract

The effect of acetyl substitution on the optical properties of cellulose acetate (CA) was investigated in the present study. During hot-stretching, the absolute orientation birefringence increased with tensile stress. The stretched films with high acetyl substitution had negative orientation birefringence, whereas those with low acetyl substitution had positive orientation birefringence. Furthermore, there was a great reduction in the rate of decrease in orientation birefringence following the cessation of hot-stretching. The slow relaxation of crystal orientation was responsible for the anomalous optical anisotropy, as confirmed by two-dimensional X-ray diffraction. Moreover, the slow relaxation of orientation birefringence would greatly benefit the preparation of CA optical retardation films by hot-stretching, because it would simplify the precise control of retardation. The stress-optical coefficient in the glassy state was also evaluated, and was found to decrease with the degree of acetyl substitution.

Keywords: Cellulose acetate; Birefringence; Orientation; Refractive index

Introduction

Because cellulose esters usually have high optical transparency and high heat resistance, they are often used for optical films such as polarizer protective films and retardation films (Edgar et al. 2004; Sata et al. 2004; Gleisser 2004; Kamide 2005; Necula et al. 2010; Yamaguchi & Mohd Edderozey 2013). Cellulose acetate (CA), which is produced by the acetylation of cellulose, is one of the most popular cellulose esters used as optical films because it is inexpensive and has excellent heat resistance. As a consequence of the rapid progression of display systems, advanced CA retardation films are currently produced by hot stretching. Multi-band waveplates, in which birefringence is proportional to wavelength, are one of the best-known examples. Mohd Edeerozey et al. (2011a) prepared a multi-band quarter-wave plate using cellulose triacetate (CTA) with a conventional plasticizer (tricresyl phosphate). Nobukawa et al. (2014) and Shimada et al. (2015) also prepared multi-band waveplates by exploiting the form birefringence of cellulose ester films.

The degree of acetyl substitution in CA has a major impact on its optical properties. Necula et al. (2010) reported that optical transparency and the refractive index are highly dependent on the degree of acetyl substitution. Yamaguchi et al. (2009) found that the degree of acetyl substitution affects the wavelength dispersion of orientation birefringence. El-Diasty et al. modified the orientation birefringence of CTA by irradiation (2007). Modification by the addition of biomass-based materials has also been proposed as a means of controlling retardation (Nobukawa et al. 2015; Soeta et al. 2017). However, the effects of the hot-stretching processing conditions remain unclear. The crystallinity of CTA increases during hot-stretching (Songsurang et al. 2012; Shimada et al. 2017). Therefore, the optimum conditions for hot-stretching should be clarified. The crystallinity of CA approximately corresponds to its acetyl content (Edgar et al. 2004; Sata et al. 2004). Therefore, in the present study the relationship between the degree of acetylation and orientation birefringence was examined by the simultaneous measurement of stress and birefringence during hot-stretching, and after the cessation of stretching. Structural change was further characterized by two-dimensional X-ray diffraction analysis. Finally, photoelastic birefringence caused by stress in the glassy state—which is an important property of optical films—was evaluated to confirm the effect of acetyl substitution.

Experimental

Samples and Film preparation

Four CA samples with various degrees of acetyl substitution were provided by the Daicel Corporation. The details of the characteristics are summarized in Table 1. The numerals in the sample code represent the degree of acetyl substitution.

Table 1 Characteristics of polymers

	Degree of acetyl substitution	M_n x 10^{-4}	M_w x 10^{-4}
CA2.9	2.93	10.0	31.8
CA2.8	2.85	11.1	35.8
CA2.4	2.44	8.3	20.7
CA2.2	2.18	7.4	20.8

Molecular weights: poly(methyl methacrylate) standard

The films were prepared by a solution-casting method as follows. Each sample was dissolved in a mixed solvent comprising dichloromethane (CH_2Cl_2) and methanol

(CH_3OH) in a 9-to-1 weight ratio, and stirred for 24 h at room temperature. The solutions were poured onto glass plates and left overnight to allow the solvent to evaporate. The obtained films (100 µm thick) were stored in a temperature- and humidity-controlled environment at 25°C and 50% relative humidity (RH) before obtaining the measurements.

Measurements

The water content of each sample film was obtained with a moisture meter (Mitsubishi Chemical, CA-200) using the Karl Fischer method, in which the Karl Fischer reagent comprising iodine, sulfur dioxide, a base, and a solvent reacts quantitatively and selectively with water (MacLeod 1991).

The refractive index of each sample film was measured as a function of wavelength using a DR-M2 Abbe refractometer (Atago). A halogen lamp with various interference filters was used, which enabled changes in wavelength, and α-bromonaphthalene was used as a contact liquid.

The temperature dependencies of tensile storage modulus E' and loss modulus E'' between 30 and 250°C were determined using an E-4000 dynamic mechanical analyzer (UBM). The frequency and heating rate were 10 Hz and 2°C/min, respectively.

Rectangular specimens (5-mm wide) were cut from solution-cast films, and uniaxially stretched beyond their glass transition temperatures; stress was measured using a tensile machine with a temperature controller (UBM, DVE-3 S1000). The initial distance between the clamps was 10 mm, and the stretching speeds were 1.0, 0.5, and 0.1 mm/min. Therefore, the initial strain rates were 0.1, 0.05, and 0.01 s^{-1}, respectively. The hot-stretching temperature was determined to show similar stress levels for all films at a constant strain rate of 0.05 s^{-1}. Optical retardation was simultaneously evaluated by measuring the light intensities under crossed polars using a polarized laser beam (632.8 nm) during stretching; the procedure has been explained in detail in the literature (Yamaguchi et al. 2012). After stretching to a draw ratio of 1.3, some of the films were used to measure the relaxation behavior of both stress and retardation by holding the stretched films at a constant temperature. The films obtained by blowing air were also used to measure the optical retardation at room temperature as a function of wavelength by changing the color filters using a KOBRA-WPR optical birefringence analyzer (Oji Scientific Instruments). Three sample films were prepared as follows: (1) cooled immediately after pre-heating prior to stretching; (2) cooled immediately after stretching to a draw ratio of 1.3; and (3) cooled over 60 s after cessation of stretching. The films were stored at 25°C and 50% RH for 1 day prior to conducting the retardation measurements.

Two-dimensional wide-angle X-ray diffraction (2D-XRD) patterns were collected with a graphite monochromatized CuKα radiation beam using an R-AXIS IIc flat imaging plate detector (Rigaku). The films were exposed for 6 min per shot in a geometrical manner by directing the X-ray beam normal to the film plane.

Stress-optical coefficients in the glassy state were evaluated as a function of wavelength at room temperature using the optical birefringence analyzer. Measurements were taken after applying various loads to the sample films.

Results and Discussion

The optical anisotropy of cellulose derivatives is affected by their water content. In general, moisture enhances the optical anisotropy of CA films (Mohd Edeerozey et al.

2011b). Therefore, the moisture content of the films was evaluated first. Figure 1 shows the water content of the films used for the optical and mechanical measurements, i.e., the samples that had been kept in a chamber at 25°C and 50% RH for 1 day. Dried films that had been kept in a vacuum oven at room temperature for 24 h were used as a reference. As expected for CA films, the moisture content, which was high in the films stored at 50% RH, decreased rapidly with the degree of acetyl substitution. Regardless of the storage conditions, the water content of the CA2.2 films was approximately twice that of the CA2.9 films.

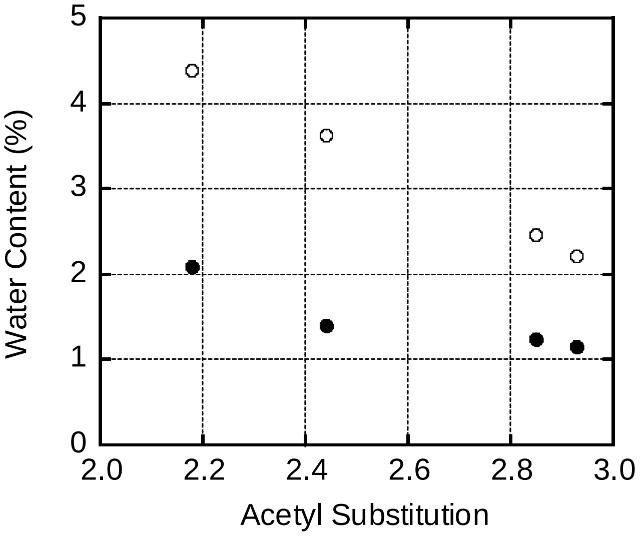

Figure 1 Water content in the CA films: (closed circles) after vacuum drying at 25°C for 24 hours and (open circles) after keeping in the temperature-and-humidity controlled chamber at 25°C and 50% RH.

The wavelength dispersion of the refractive index is shown in Figure 2 for the vacuum-dried and moisture-controlled (25°C, 50% RH) samples. The refractive index decreased with increasing acetyl substitution, whereas the wavelength dispersion was barely affected. Figure 3 represents the relationship between the degree of acetyl substitution and the refractive index at 589 nm (D-line). The refractive index decreased linearly with the degree of acetyl substitution in the dried samples. In contrast, the refractive index increased in the moisture-controlled samples, and the increase was most pronounced in CA2.2. The increase in the refractive index can be attributed to the absorbed water, which is an interesting phenomenon. Considering that the refractive index of water is 1.333, the simple addition of the refractive indices of the individual components—i.e., CA and water—cannot account for the refractive index observed. The polarizability of CA would be enhanced by the strong hydrogen bonding with water molecules.

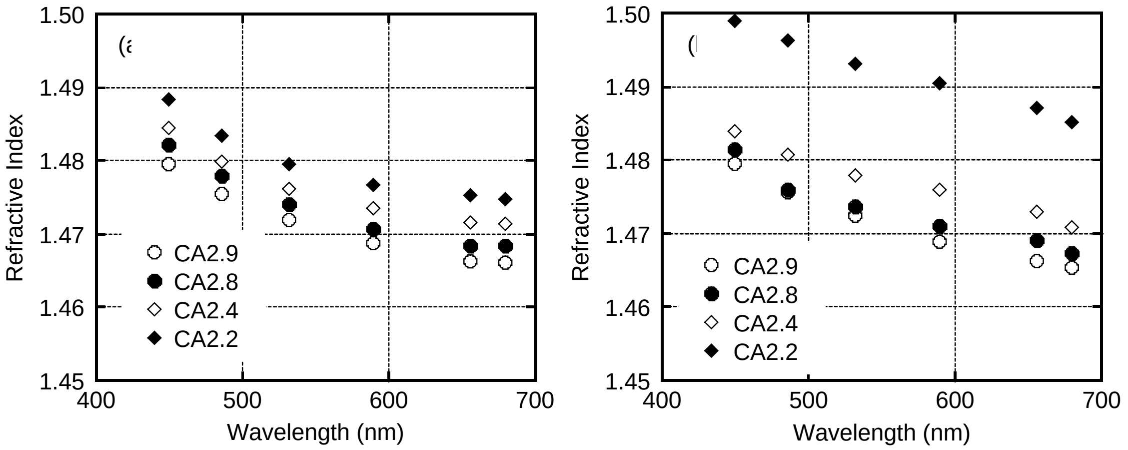

Figure 2 Wavelength dispersion of refractive index for (a) vacuum-dried films and (b) moisture-controlled films at 25°C and 50% RH.

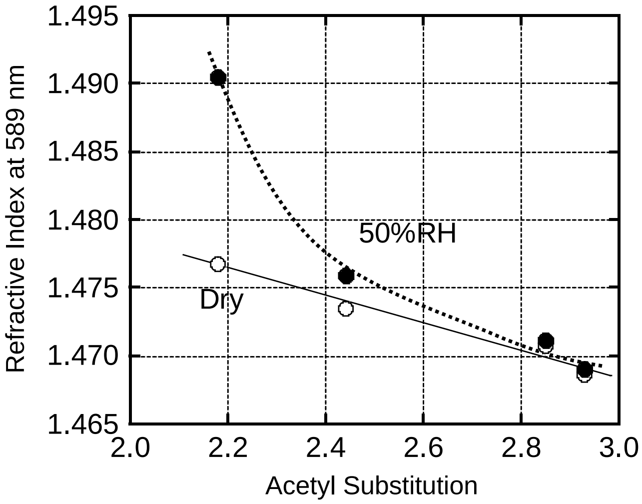

Figure 3 Relation between acetyl substitution and refractive index at 589 nm for (open circles) vacuum-dried films and (closed circles) moisture-controlled films at 25^{o}C and 50% RH.

Figure 4 shows the temperature dependence of the tensile storage modulus E' and the loss modulus E''. Both CA2.2 and CA2.4—i.e., the samples with low acetyl substitutions—exhibited a rapid decrease in E', which can be attributed to the glass-to-rubber transition. In contrast, the E' curve for the other samples—i.e., CA2.8 and CA2.9—featured a plateau, even beyond the glass transition temperature T_g. This was expected because the crystallites act as crosslink points. In other words, a high degree of acetyl substitution increased the crystallinity of the CA films, as reported previously (Edgar et al. 2001; Sata et al. 2004), although the films were transparent. The E' curve for CA2.8 exhibited a slight increase beyond 210°C. This can be attributed to cold crystallization. Because the solution-cast film had a low degree of crystallinity, further crystallization occurred beyond T_g. A similar behavior was detected in CA2.4 at approximately 230°C, indicating that CA2.4 was crystalline, as explained in detail later. The peak temperature in the E'' curve, defined as T_g in the present study, decreased slightly with increasing degree of acetyl substitution: 216°C for CA2.2, 207°C for CA2.4, 199°C for CA2.8, and 198°C for CA2.9.

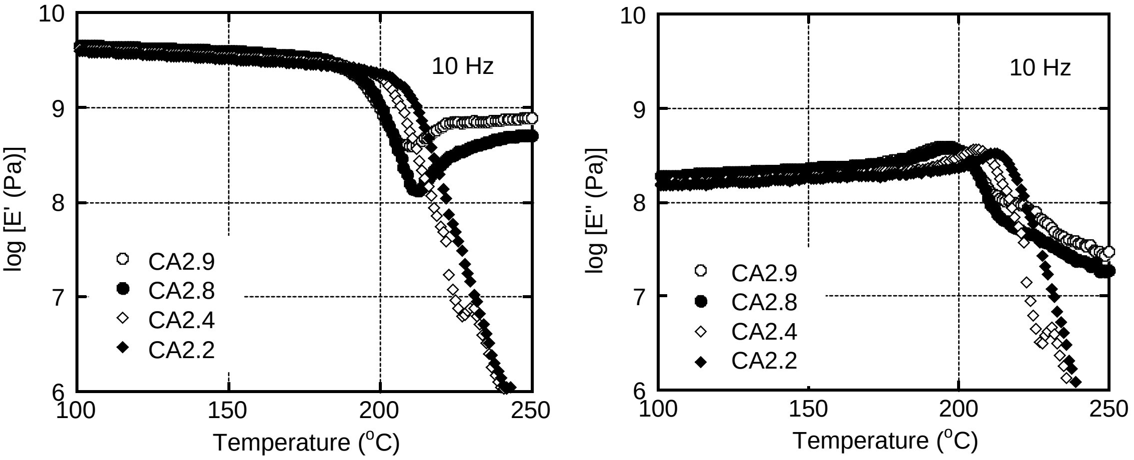

Figure 4 Temperature dependence of dynamic tensile moduli (a) storage modulus *E’* and (b) loss modulus *E”*.

The engineering tensile stress and orientation birefringence growth curves for CA2.9 during hot-stretching are shown in Figure 5. The birefringence was negative, as reported previously (El-Diasty et al. 2007; Yamaguchi et al. 2009). The stress level increased with increasing strain rate, which is the typical mechanical behavior of a viscoelastic body. Because the degree of main-chain orientation dictates the stress in the rubbery region, films stretched at the highest strain rate (0.1 s^{-1}) had the highest orientation birefringence. It should be noted that the orientation birefringence, which is in general determined by the product of the intrinsic birefringence and the orientation function, was hardly affected by the strain rate, i.e., the stress level. The result demonstrated that the stress-optical law in the rubbery region (Kuhn & Grün 1942) was not applicable to sample CA2.9.

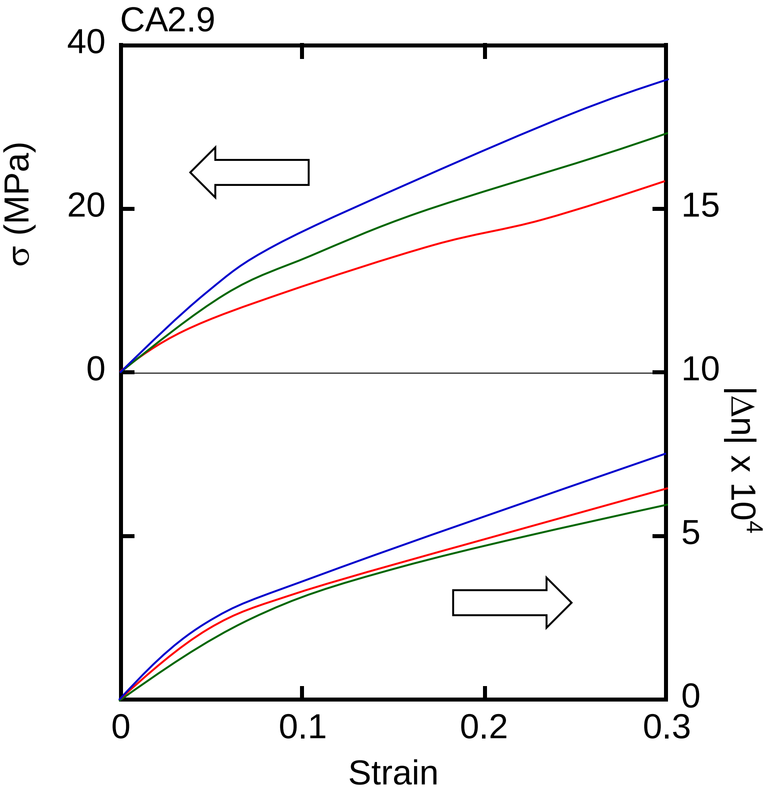

Figure 5 Growth curves of the tensile stress σ and orientation birefringence Δn during stretching for CA2.9 at various strain rates. The sign of birefringence was negative.

The stress and birefringence decay curves during relaxation, and following the cessation of stretching at a draw ratio of 1.3 (applied at 0.05 s^{-1}) were evaluated for CA2.9 and CA2.4. As shown in Figure 6, the birefringence ($t > 0$) did not decrease much in either sample, although the stress dropped off rapidly. The results also demonstrated that the stress-optical rule was not applicable to the CA samples. This anomalous and interesting behavior indicates that the crystalline regions of CA, which barely exhibit orientation relaxation, are responsible for the orientation birefringence, as discussed later. From an industrial perspective, this is a great advantage, because it is easy to provide appropriate retardation by hot-stretching CA films, owing to the slow relaxation of birefringence after stretching ceases.

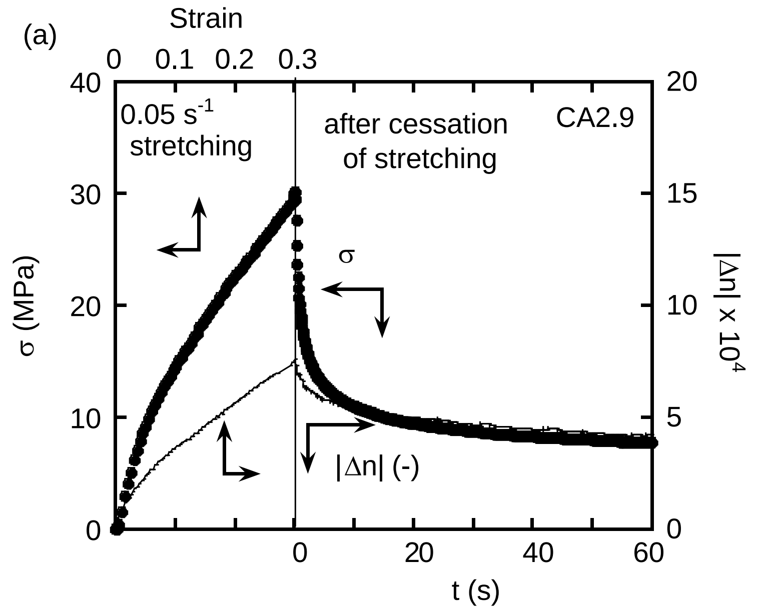

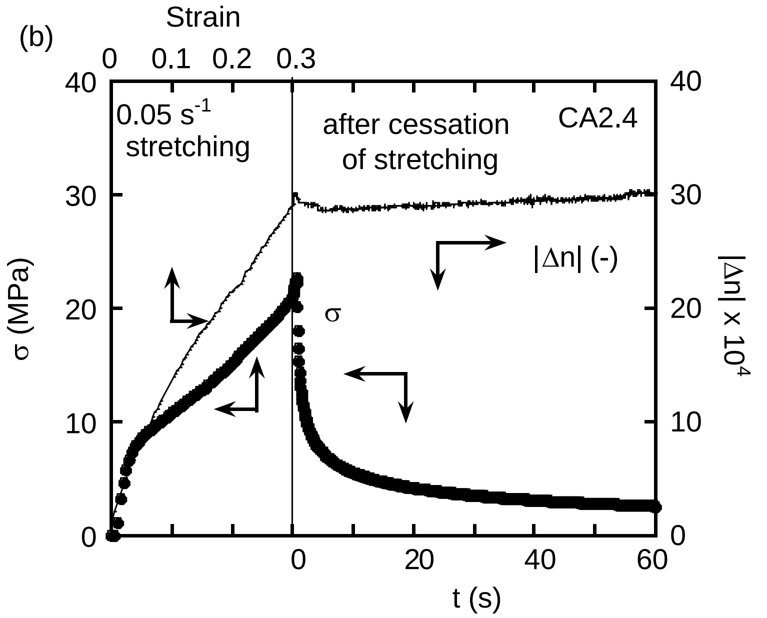

Figure 6 Growth curves of the tensile stress σ and orientation birefringence Δn during stretching at 0.05 s^{-1} and after cessation of stretching at a draw ratio of 1.3 for (a) CA2.9 and (b) CA2.4. The sign of the birefringence was denoted in the parenthesis.

The films that had been stretched at 0.05 s^{-1} were cooled by blowing air after the relaxation process (60 s after the cessation of stretching), and the chucks were removed from the tensile machine to evaluate the wavelength dispersion of birefringence. The same measurements were performed using the stretched films cooled immediately after the cessation of stretching without relaxation. The results are shown in Figure 7. The birefringence of the films pre-heated at the stretching temperature prior to stretching is also shown as "before stretching" in Figure 7 (no birefringence). Because the measurements were performed at room temperature after cooling, the birefringence of the stretched films shown in Figure 7 is slightly different from the data in Figures 5 and 6. As seen in Figure 7, we confirmed that there was hardly any relaxation of orientation birefringence in any of the samples. CA2.8 exhibited negative and markedly low orientation birefringence with strong wavelength dispersion. In contrast, CA2.4 and CA2.2 exhibited large and positive orientation birefringence values with weak wavelength dispersion. Furthermore, CA2.4 and CA2.2 exhibited unusual wavelength dispersion; i.e., the birefringence increased with the wavelength. This phenomenon can be explained by the sum contributions of the hydroxyl and acetyl groups (Yamaguchi et al. 2009).

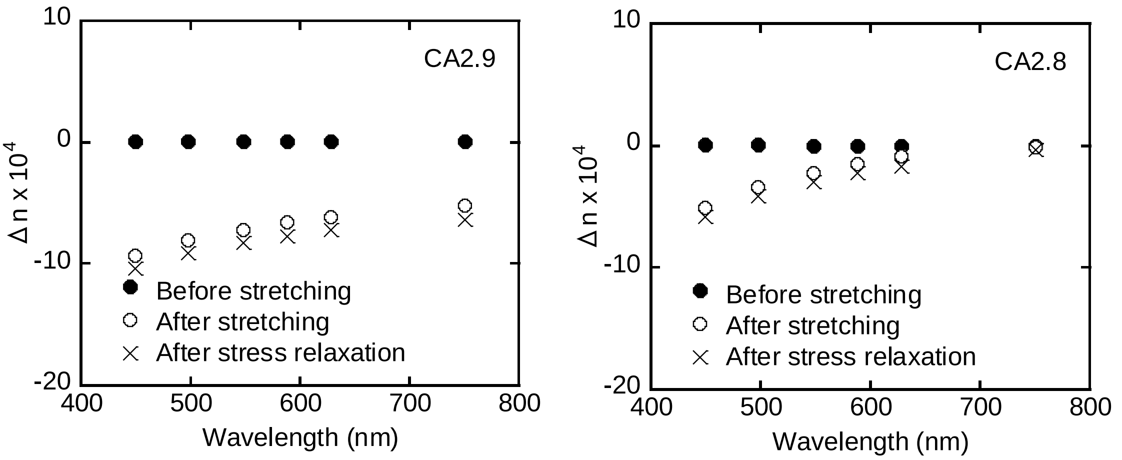

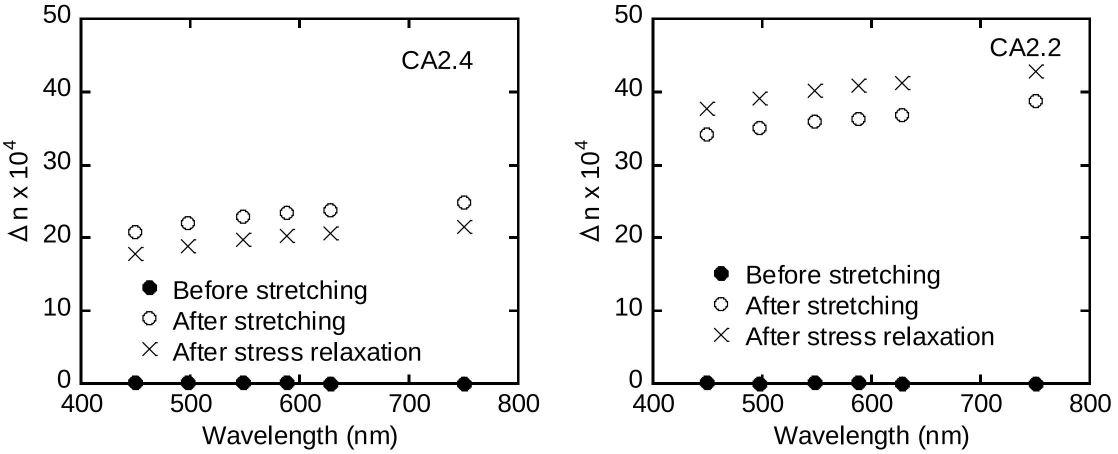

Figure 7 Wavelength dispersion of the orientation birefringence for the films: (closed circles) after pre-heating prior to stretching, (open circles) immediately after stretching without relaxation process, and (x) after the relaxation process (60 sec after cessation of stretching). (a) CA2.9, (b) CA2.8, (c) CA2.4, and (d) CA2.2.

The orientation birefringence at 589 nm is plotted as a function of the degree of acetyl substitution in Figure 8. The values were measured at room temperature using the unrelaxed stretched films. The orientation birefringence increased monotonically with an increasing number of hydroxyl groups, i.e., low acetyl substitution. This is due to the strongly anisotropic polarizability arising from the hydroxyl groups in a stretched film. The direction of the polarizability anisotropy for the samples having a high degree of acetyl substitution was perpendicular to that of the polymer chain; i.e., the acetyl groups contribute negative birefringence. Figure 8 indicates that a CA sample with an appropriate acetyl substitution that is close to 2.8 is free from orientation birefringence.

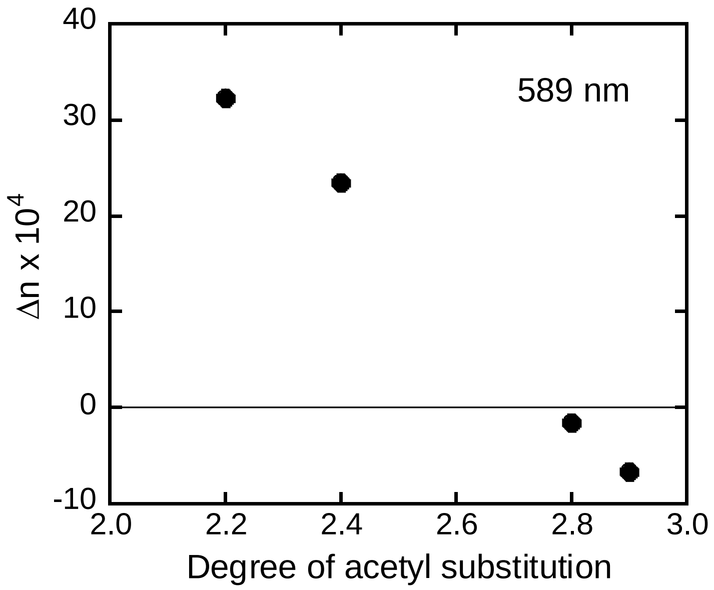

Figure 8 Orientation birefringence at 589 nm as a function of the acetyl substitution. The values were measured at room temperature using the stretched films without relaxation process.

Figure 9 shows the 2D-XRD images of the through views of CA2.4 films: (a) a solution-cast film; (b) a film after pre-heating prior to stretching; (c) a film after stretching at 0.05 s^{-1} without relaxation; and (d) a film after relaxation for 60 s. There were two noticeable rings in the 2D-XRD images of the solution-cast film. These diffraction peaks are attributable to the (010) and (020) planes, respectively (Roche et al. 1978; Siroski et al. 2013). The peak intensities increased slightly following pre-heating because of crystallization. After stretching, the peaks were clearly visible on the equator because the polymer chains orient to the stretching direction. Moreover, the peaks did not diminish even after relaxation, demonstrating that the orientation of the crystalline phase remained. The result suggests that the orientation of amorphous chains does not play an important role in birefringence, although the stress in the rubbery state is governed by the orientation of amorphous chains (Read 1975).

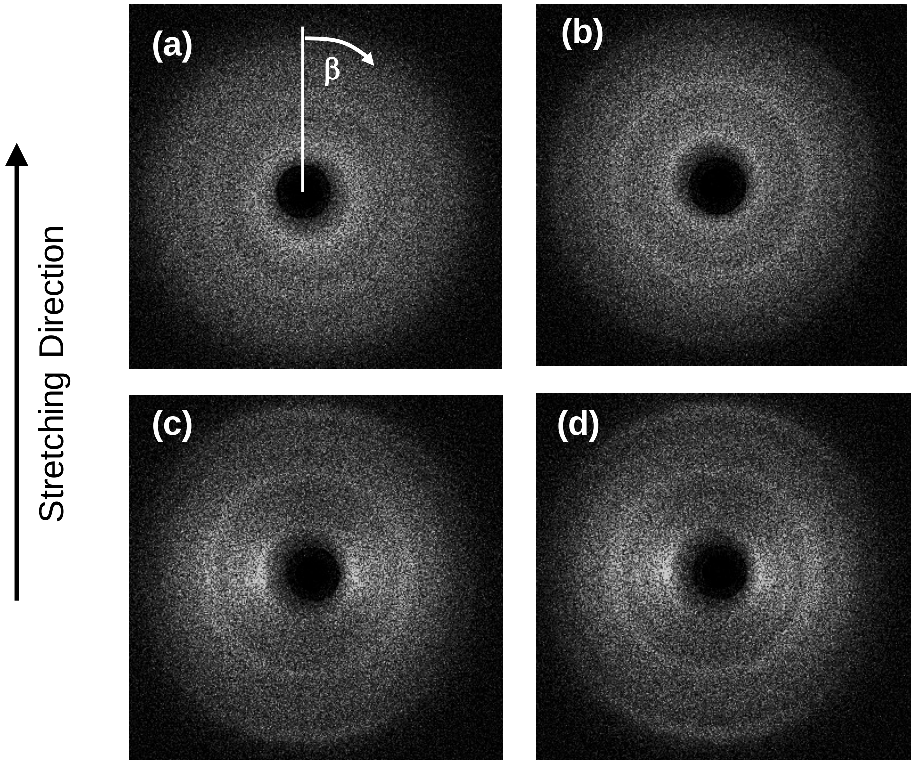

Figure 9 2D-XRD profiles of CA2.4: (a) solution-cast film, (b) after pre-heating prior to stretching, (c) immediately after stretching without relaxation process, and (d) after the stress relaxation process (60 sec after cessation of stretching).

Figure 10 shows the azimuthal intensity distribution at $2\theta = 7.8°$, i.e., the (010) plane, for all CA samples. The strongest peaks were detected on the equator, i.e., β = 90 and 270°, revealing the chain orientation in the crystals. The figures demonstrate that there was hardly any orientation relaxation of the crystalline chains in any of the samples including CA2.2, i.e., the sample with low crystallinity.

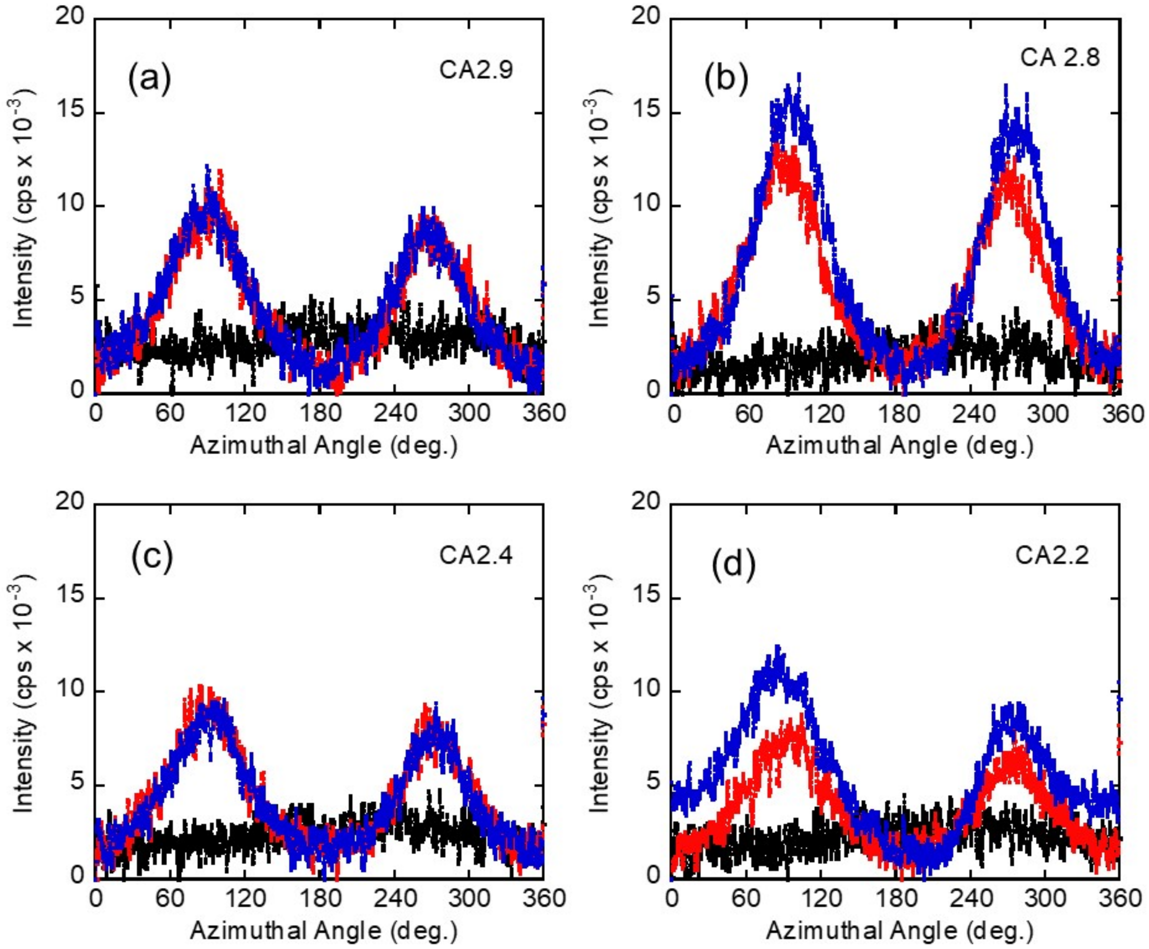

Figure 10 Azimuthal intensity distributions at $2\theta = 7.8°$, i.e., the (010) plane of (a) CA2.9, (b) CA2.8, (c) CA2.4, and (d) CA2.2; (black) after pre-heating prior to stretching, (red) immediately after stretching without relaxation process, and (blue) after the relaxation process (60 sec after cessation of stretching).

The stress-optical coefficient in the glassy state C_G was shown in Figure 11, which was evaluated by the relationship between the applied load and the retardation at room temperature. It was confirmed that the birefringence was proportional to the applied stress; i.e., the stress-optical law in the glassy region was applicable to all CA films. The stress-optical coefficient, i.e., the slope of the birefringence – stress relation, decreased with increasing the acetyl substitution. Furthermore, all films exhibited weak and ordinary wavelength dispersion. The absolute value of CA2.9 was almost similar to those of poly(methyl methacrylate) and polystyrene, and much lower than that of polycarbonate (Liu et al. 1996; Okita et al. 2005; Szczurowski et al. 2010).

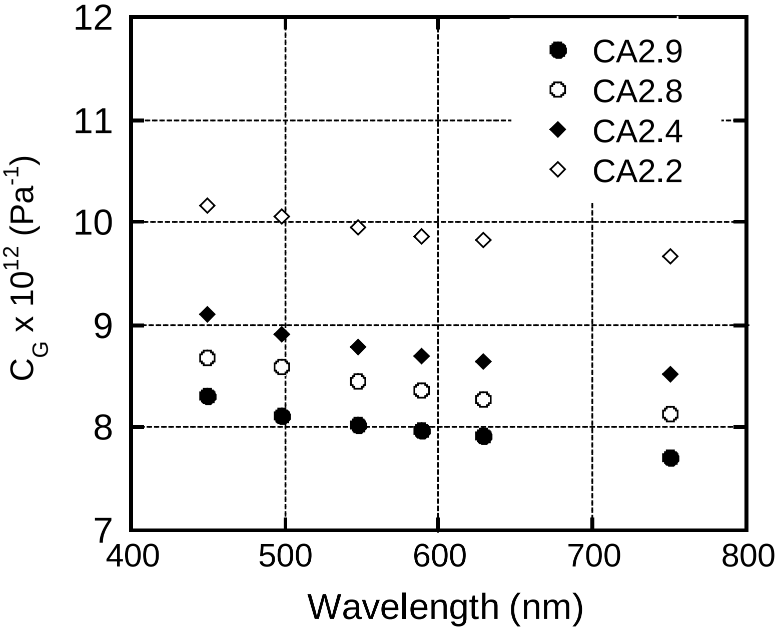

Figure 11 Wavelength dispersion of the stress-optical coefficient C_G in the glassy region.

Conclusion

The optical anisotropy was studied using various CA samples with different degrees of acetyl substitution. As increasing the acetyl substitution, the orientation birefringence decreased. Furthermore, the orientation birefringence was found to be determined mainly by the orientation of crystalline region, which was revealed by

2D-XRD measurements. As a result, the birefringence showed slow relaxation after the cessation of hot-stretching. This anomalous behavior will be a great benefit for CA because the retardation is not sensitive to the cooling condition at hot-stretching process. The stress-optical coefficient in the glassy region was found to decrease with the acetyl substitution. The value of CA with a large amount of acetyl substitution is similar to those of poly(methyl methacrylate) and polystyrene.

Acknowledgement

A part of this work was supported by JSPS Grant-in-Aid for Scientific Research (B) Grant Number 16H04201. The authors would like to express their sincere gratitude to Daicel Corporation for their valuable suggestions and the kind supply of the samples employed in this study.

References

Edgar KJ, Buchanan CM, Debenham JS, Rundquist PA, Seiler BD, Shelton MC, Tindall D (2001) Advances in cellulose ester performance and application. Prog. Polym. Sci. 26:1605-1688.

El-Diasty F, Soliman MA, Elgendy AFT, Ashour A (2007) Birefringence dispersion in uniaxial material irradiated by gamma rays: cellulose triacetate films. J Opt A Pure Appl Opt 9(3):247-252.

Glasser WG (2004) Prospects for future applications of cellulose acetate. Macromol Symp 208(1):371-394.

Kamide K (2005) Cellulose and cellulose derivatives, Elsevier Science: Amsterdam.

Kuhn W, Grün F (1942) Beziehungen zwishen elastischen konstanten und dehnungsdoppelbrechung hochelastischer stoffe. Kolloid-Z 101(3):248-271.

Ryu DS, Inoue T, Osaki K (1996) A simple evaluation method of stress-optical coefficient of polymers. Nihon Reoroji Gakkaishi 24(3):129-132.

MacLeod SK (1991) Moisture determination using Karl Fischer titrations. *Anal. Chem.* 63:557A-566A.

Mohd Edeerozey AM, Tsuji M, Nobukawa S, Yamaguchi M (2011a) Effect of moisture on the orientation birefringence of cellulose esters. Polymers 3(2):955-966.

Mohd Edeerozey AM, Tsuji M, Shiroyama Y, Yamaguchi M (2011b) Wavelength dispersion of orientation birefringence for cellulose esters containing tricresyl phosphate. Macromolecules 44(10):3942-3949.

Necula AM, Olaru N, Olaru L, Homocianu M, Ioan S (2010) Influence of the substitution degrees on the optical properties of cellulose acetates. J Appl Polym Sci 115:1751-1757.

Nobukawa S, Shimada H, Aoki Y, Miyagawa A, Vu Ahn D, Yoshimura H, Tachikawa Y, Yamaguchi M (2014) Extraordinary wavelength dispersion of birefringence in cellulose triacetate film with anisotropic nanopores. Polymer 55:3247-3253.

Nobukawa S, Enomoto-Rogers Y, Shimada H, Iwata T, Yamaguchi M (2015) Effect of acetylation site on orientation birefringence of cellulose triacetate. Cellulose 22(5):3003-3012.

Ohkita H, Ishibashi K, Tsurumoto D, Tagaya A, Koike Y (2005) Compensation of the photoelastic birefringence of a polymer by doping with an anisotropic molecule, Appl Phys A Mater Sci Process 81:617 – 620.

Read BE (1975) Structure and properties of oriented polymers, Ed. Ward IM. Applied Science Publishers, London, Chap. 4.

Roche E, Chanzy H, Boudeulle M, Marchessault RH, Sundararajanid E (1978) Three-dimensional crystalline structure of cellulose triacetate II, Macromolecules 11(1):86-94.

Sata H, Murayama M, Shimamoto S (2004) Properties and applications of cellulose triacetate film. Macromol Symp 208(1):323-333.

Shimada H, Nobukawa S, Yamaguchi M (2015) Development of microporous structure and its application to optical film for cellulose triacetate containing diisodecyl adipate. Carbohydrate Polymers 120:22-28.

Shimada H, Kiyama A, Phulkerd P, Yamaguchi M (2017) Anomalous optical anisotropy of oriented cellulose triacetate film. J. Soc. Rheol. Jpn. 45(1):29-34.

Sikorski P, Wada M, Heux L, Shintani H, Stokke BT (2013) Crystal structure of cellulose triacetate I. Macromolecules 37(12):4547-4553.

Soeta H, Fujisawa S, Saito T, Berglund L, Isogai A (2015) Low-birefringent and highly tough nanocellulose-reinforced cellulose triacetate. ACS Appl Mater Interfaces 7(20):11041-11046.

Songsurang K, Mohd Edeerozey AM, Miyagawa A, Phulkerd P, Nobukawa S, Yamaguchi M (2013) Optical anisotropy in solution-cast film of cellulose triacetate.

Cellulose 20(1):83-89.

Szczurowski MK, Martynkien T, Statkiewicz-Barabach G, Khan L, Webb DJ (2010) Measurements of stress-optic coefficient in polymer optical fibers. Opt. Lett. 35(12):2013-2015.

Yamaguchi M, Okada K, Mohd Edeerozey AM, Shiroyama Y, Iwasaki T, Okamoto K (2009) Extraordinary wavelength dispersion of orientation birefringence for cellulose esters. Macromolecules 42(22):9034-9040.

Yamaguchi M, Mohd Edeerozey AM, Songsurang K, Nobukawa S (2012) Material design of retardation films with extraordinary wavelength dispersion of orientation birefringence: a review. Cellulose 19:601-613

Yamaguchi M, Mohd Edeerozey AM (2013) Optical properties of cellulose-esters and application to optical functional films in "Pulp production and processing: from papermaking to high-tech products", Ed. Pope V, pp.391-411, Smithers Rapra, Akron.